H1prelim-08-033 Submitted to

XVI International Workshop on Deep-Inelastic Scattering, DIS2008, April 7-11, 2008, London
Parallel Session **Hadronic Final States and QCD**

Electronic Access:https://www-h1.desy.de/publications/H1preliminary.short_list.html

Prompt Photon Production in Photoproduction at HERA

H1 Collaboration

Abstract

A measurement of prompt photons in photoproduction in ep collisions with the H1 detector is presented. The analysis is based on the data taken in the years 2004-2007, corresponding to a total integrated luminosity of $340\,\mathrm{pb}^{-1}$. The photon signal is extracted using a multivariate analysis based on calorimeter cluster different shower shape variables. Inclusive and exclusive cross sections are presented as a function of the transverse energy E_T^{γ} in the range 5 to $15\,\mathrm{GeV}$ and the pseudorapidity η^{γ} in the range -1.0 to 2.4. The momentum fractions x_{γ} and x_{proton} of the incident photon and proton carried by the constituents participating in the hard scattering process are measured as well. The results are compared to predictions from theoretical calculations.

1 Introduction

Isolated photons with high transverse momentum in the final state are a direct probe of the dynamics of the hard subprocess in ep collisions. The measurement provides complemantary information to the study of jet production with different and generally lower corrections for hadronisation. The process gives access to parton density functions of both photon and proton. The ZEUS collaboration has reported measurements of prompt photon production [1–3]. The H1 collaboration has performed a measurement of prompt photon cross section both in photoproduction [4] and in Deep Inelastic Scattering [5]. Comparison to LO and NLO calculations showed that cross sections in DIS are significantly underestimated. In photoproduction, the inclusive cross section is slightly underestimated by the calculations but the photon plus jet cross section is described reasonably well.

The present preliminary analysis extends the phase space of the previous measurement in photoproduction towards larger pseudorapidities of the photon and lower event inelasticities. The data used for the measurement have been collected by the H1 detector during the years 2004-2007 corresponding to a total integrated luminosity of $340\,\mathrm{pb}^{-1}$, increased by a factor of three over previous measurement.

2 Experimental Method

Photons are reconstructed as a compact electromagnetic cluster in the liquid argon calorimeter (LAr) [6]. The transverse energy of the cluster is restricted to 5 GeV$< E_T^\gamma < 15\,$GeV and the pseudorapidity region of $-1.0 < \eta^\gamma < 2.4$. The main experimental difficulty is the separation of the photons from neutral mesons, mainly π^0 or η, decaying into multi-photon final states. The number of photons is extracted using a multivariate analysis (MVA) [7] based on six discriminating shower shape variables. The final cross sections are corrected for detector effects using prompt photon Monte Carlo events.

Events are triggered by a high energy LAr cluster. Low Q^2 DIS events are removed by excluding events with an electron in the backward calorimeter (SpaCal). The inelasticity is restricted to $0.1 < y_h = \Sigma(E - p_z)/2E_e < 0.7$ where E_e is the energy of the incoming electron and the sum runs over the energy (E) and the longitudinal momentum (p_z) of all final state particles. The z-position of the event vertex is required to be within 40 cm of the nominal vertex position. In order to correctly determine the vertex position at least two well reconstructed central tracks are required. At least one jet with transverse momentum larger than $3.5\,$GeV is required. The jet is reconstructed using the k_T algorithm [12] with cone size $R_0 = 1$ running over all final state particle candidates, including photon candidates.

Photon candidates are defined by electromagnetic clusters with transverse energy $5 < E_T^\gamma < 15\,$GeV and pseudorapidity $-1.0 < \eta^\gamma < 2.4$. Candidates close to the cracks of the calorimeter are rejected. Charged particles are removed by a combined condition based on the information from the Central Tracking Detector (CTD) and the Central Inner Proportional chamber (CIP) [8]. The cluster has to be compact with a transverse radius of less than 6 cm. In order to suppress background the photon needs to be isolated, what is achieved by a cut on the fraction of the transverse energy of the jet containing the photon carried by the photon, $z = E_T^\gamma / E_T^{photon-jet} > 0.9$. The invariant mass of the cluster, when combined with the closest neighbouring electromagnetic cluster with an energy larger than 80 MeV must be larger than 0.3 GeV. This last requirement rejects candidates from π^0 decays with two photons reconstructed in separated clusters.

For the exclusive selection of a photon accompanied by a jet, the selection on the transverse momentum of the jet larger than 4.5 GeV and pseudorapidity $-1.3 < \eta^{jet} < 2.4$ is performed.

For both inclusive and exclusive selections the photon signal is extracted by a MVA using the shower shape variables.

2.1 Extraction of the photon signal and systematic errors

Six different shower shape variables are used to discriminate between photons and neutral mesons [5].

- Hot core fraction: fraction of energy deposited in four or eight - depending on the granularity of the calorimeter - contiguous cells including the cell with the highest energy.
- Transverse radius of the cluster, where the transverse plane is perpendicular to the direction of the incoming particle.
- Energy fraction deposited in the hottest cell of the cluster.
- Energy fraction deposited in the first layer of the LAr.
- Transverse kurtosis giving the information how strongly the energy distribution is peaked.
- Transverse symmetry, defined as the ratio of the spread of the transverse cell distributions along the two principal axes.

The discrimination power between the prompt photon signal (photons coming from direct events, from resolved and photons radiated off the quark) and the background (di-jet production events) can be seen in figure 1. The plot shows the distribution of six different shower shape variables for the photon candidate clusters compared to the PYTHIA predictions for the signal (scaled to the measured cross section) and the background. The transverse radius and the hot core fraction exhibit the best discrimination power, as can be seen by comparing the prompt photon signal (photons coming from direct events, from resolved and photons radiated off the quark) to the background (di-jet production events) distributions.

The variables are combined in a MVA producing a final discriminator in bins of transverse energy E_T^γ and pseudorapidity η^γ. The signal content is obtained by fitting the discriminator distributions of pure signal and pure background samples of single particle Monte Carlo to the data. As an example for the fit figure 2 shows the discriminator for six different energy bins for one η^γ bin. The figures show the signal and background distributions together with the data.

Various systematic uncertainties were considered. The total systematic error per bin is obtained by adding all different systematic errors in quadrature. The dominant errors are listed below.

- Description of the shower shape variables in the simulation. Systematic shift of shower shape variables between 3.5% and 8% (depending on the variable and pseudorapidity region) motivated by previous study [5] leads to errors up to 30% on the cross sections.
- The uncertainty of the description of the trigger correction together with the steep slope of the trigger efficiency at low transverse energies leads to a systematic error up to 20% in the lowest E_T^γ bin.
- The model dependence was studied by comparing acceptance corrections obtained with HERWIG and PYTHIA, leading to a systematic error of up to 10% in the most forward η^γ bin.
- Description of the photon conversion rate in the detector. A variation of the conversion rate by factors 0.5 and 1.5 leads to a systematic error of 15% in the most forward η^γ bin.
- From the difference between the single particle simulations and the PYTHIA simulation including the simulation of full hadronic final state systematic error of 5% (15% in the most forward η^γ bin) is assigned.

3 Monte Carlo simulation and calculations

Monte Carlo (MC) simulations are used in this analysis for the determination of the detector acceptance and for the extraction of the photon signal. The acceptance correction is determined from events generated with PYTHIA 6.2 [9] event generator. The simulated signal contains contributions from direct and resolved production of prompt photons as well as photons radiated from the quark in di-jet events. The background sample contains genuine di-jet events without high energetic photons from the quark. For the extraction of the photon signal using shower-shape-based MVA high statistics single particle Monte Carlo samples are used. They consist of single photons (signal part) and single hadrons (mainly π^0 and η - background part). All generated events are passed through a full GEANT [10] simulation of the H1 detector and through the same reconstruction and analysis program as used for the data.

All the results are compared to two sets of calculations corrected to hadron level and multiple interactions:

- The FGH (Fontannaz-Guillet-Heinrich) [13, 14] calculation includes NLO corrections to the direct and resolved photon production as well as contribution from quark-to-photon fragmentation and the direct box diagram $\gamma g \to \gamma g$ which is calculated to order α_s^2. The error is evaluated by varying the fragmentation and renormalisation scales together by a factor 0.5 and 2.0 leading to overall error of at most 10%.
- The ZL (Zotov-Lipatov) [15] calculation is based on the k_T factorisation approach and uses the unintegrated quark and gluon densities of the proton and the photon according to the Kimber-Martin-Ryskin prescription. Direct and resolved contributions are taken into account. Estimation of the error has been performed by multiplying the p_T^2 scale by a factor 4 and $1/4$ leading to an error of at most 10%.

4 Results

Differential cross sections for the production of prompt photons in photoproduction are measured for $Q^2 < 1\,\mathrm{GeV}^2$, $0.1 < y_h < 0.7$ for photons with $5 < E_T^\gamma < 15\,\mathrm{GeV}$, pseudorapidity $-1.0 < \eta^\gamma < 2.4$ and the transverse energy fraction $z = E_T^\gamma / E_T^{photon-jet} > 0.9$.

Figure 3 shows the single differential inclusive cross sections as a function of transverse energy and the pseudorapidity of the photon. Both calculations are slightly lower than the data most significantly at low E_T^γ.

Exclusive (photon plus jet) single differential cross sections measurement as a function of transverse energy and pseudorapidity of the photon (figure 4), transverse momentum and pseudorapidity of jet (figure 5) and momentum fractions x_γ^{obs} and x_{proton}^{obs} (figure 6) show better agreement with the calculations. The largest discrepancy arises for the highest bin in x_γ^{obs}, where both calculations give different prediction, while data does not favour any of them.

5 Conclusions

Results on both inclusive and exclusive prompt photon production in photoproduction as measured by the H1 collaboration have been presented. The measurement has been compared to two calculations, one using a collinear approach and the other based on k_t factorisation. The predictions for the inclusive sample are slightly lower than the data, most significantly at low E_T^γ but there is reasonable agreement for the photon plus jet sample except at high x_γ^{obs}

References

[1] J. Breitweg *et al.* Physics Letters B 472 (2000) 1-2, 175-188 [arXiv:hep-ex/9910045]

[2] S. Chekanov *et al.* [ZEUS Collaboration], Phys.Lett. B511 (2001) 19-32 [arXiv:hep-ex/0104001]

[3] S. Chekanov *et al.* [ZEUS Collaboration], Eur.Phys.J. C49 (2007) 511-522 [arXiv:hep-ex/0608028]

[4] A. Aktas *et al.* [H1 Collaboration], Eur. Phys. J.**C38** (2005) 437 [arXiv:hep-ex/0407018].

[5] F.D.Aaron *et al.* [H1 Collaboration], 0711.4578 [hep-ex].

[6] B. Andrieu *et al.* [H1 Calorimeter Group Collaboration], Nucl. Instrum. Meth. A**336** (1993) 460.

[7] J. Friedman, T. Hastie and R. Tibshirani, The Elements of Statistical Learning, Springer Series in Statistics, 2001

[8] J. Becker *et al.*, Nucl. Instrum. Meth. A **586** (2008) 190 [arXiv:physics/0701002].

[9] T. Sjöstrand *et al.*, PYTHIA 6.2 Physics and Manual [hep-ph/0108264].

[10] GEANT 3, R.Brun *et al.*, CERN_DD/EE/84-1.

[11] I. Abt *et al.* [H1 Collaboration] Nucl. Instr. and Meth. **A 386** (1997) 310, ibid, 348.

[12] Stephen D. Ellis, Davison E. Soper, Phys.Rev. **D48** (1993) 3160 [hep-ph/9305266].

[13] M. Fontannaz, J. P. Guillet and G. Heinrich, Eur. Phys. J. C **21** (2001) 303 [arXiv:hep-ph/0105121].

[14] M. Fontannaz and G. Heinrich, Eur. Phys. J. C **34**, 191 (2004) [arXiv:hep-ph/0312009].

[15] A. V. Lipatov and N. P. Zotov, Phys. Rev. D **72** (2005) 054002 [arXiv:hep-ph/0506044].

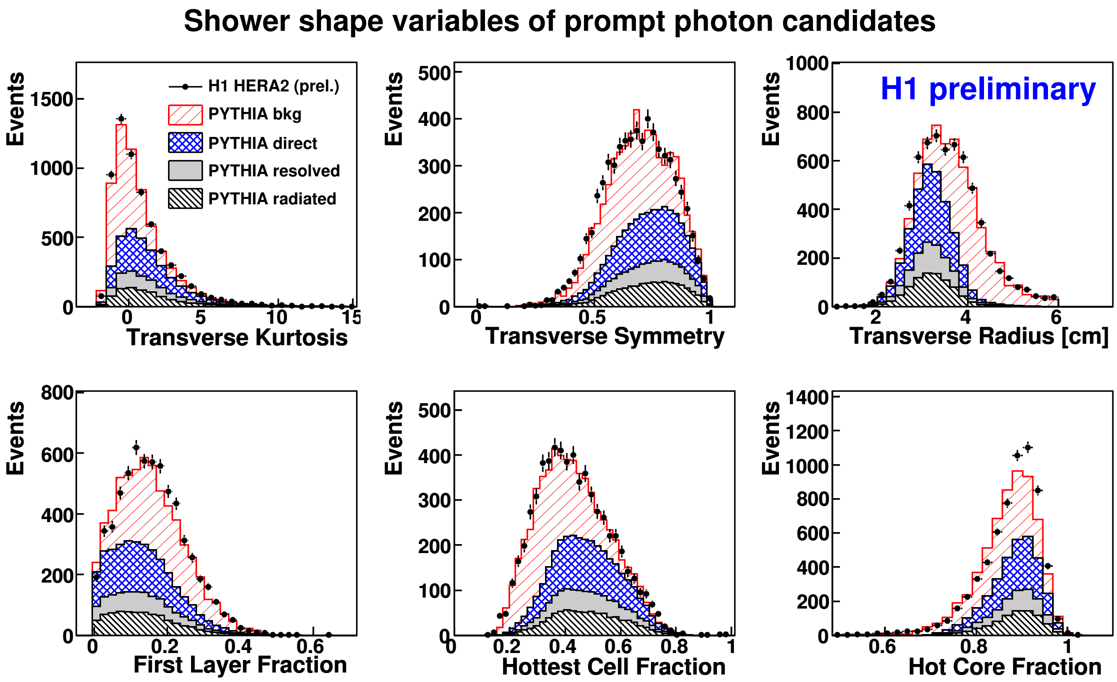

Figure 1: Shower shape variables used to discriminate between photons and neutral mesons: transverse kurtosis, transverse symmetry, transverse radius, energy fraction in the first layer, energy fraction in the hottest cell and energy fraction in the hot core of cluster. The measured data points are shown together with the radiated, resolved and direct signal Monte Carlo and remaining background, as estimated by PYTHIA. The MC prediction is scaled to the measured cross section.

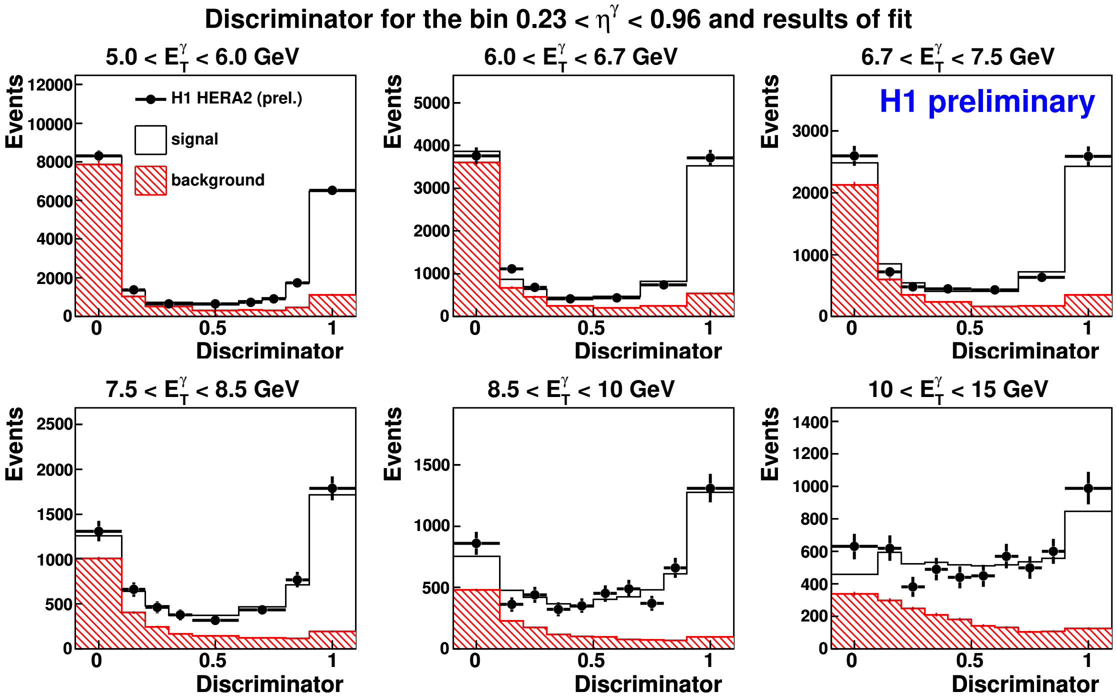

Figure 2: Examples of the MVA discriminator distributions: η^γ bin $0.23 < \eta^\gamma < 0.96$ and six transverse energy intervals. The fitted distributions of the single particle signal and background are also shown.

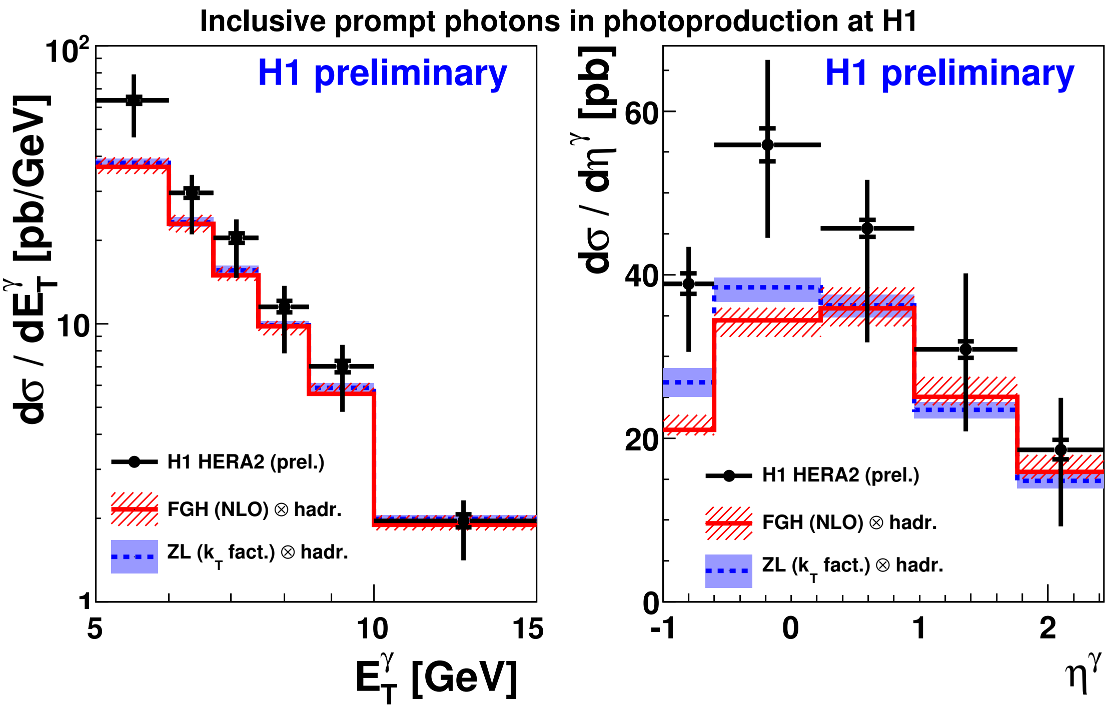

Figure 3: Inclusive prompt photon single differential cross sections as function of E_T^γ (left) and η^γ (right). The cross sections are measured in visible range defined by $5 < E_T^\gamma < 15\,\text{GeV}$, $Q^2 < 1\,\text{GeV}^2$, $0.1 < y_h < 0.7$ and $z = E_T^\gamma / E_T^{photon-jet} > 0.9$. The inner errors in the figures represent the statistical errors, while the outer are the statistical and the systematical errors added in quadrature. The measured cross section is compared to the Fontannaz-Guillet-Heinrich (continuous red) and Zotov-Lipatov (dashed blue) calculations.

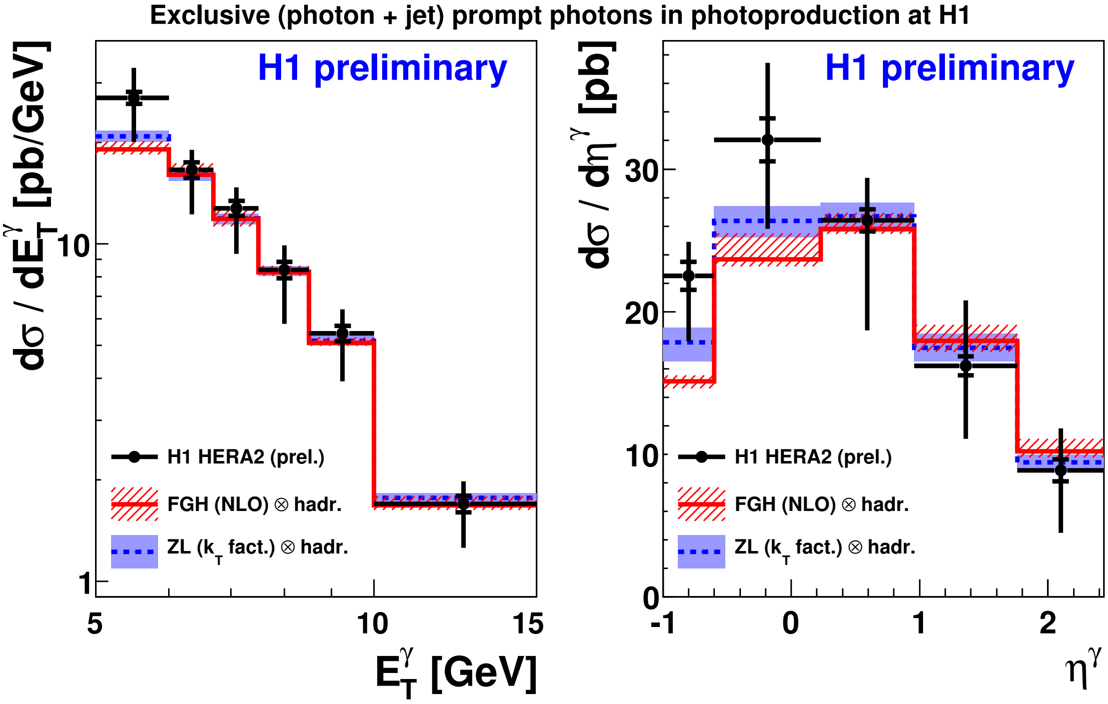

Figure 4: Exclusive prompt photon single differential cross sections as function of E_T^γ (left) and η^γ (right). The cross sections are measured in range defined in caption of figure 3. In addition jet with transverse momentum $p_T^{jet} > 4.5\,\mathrm{GeV}$ and pseudorapidity $-1.3 < \eta^{jet} < 2.4$ is required. The inner errors in the figures represent the statistical errors, while the outer are the statistical and the systematical errors added in quadrature. The measured cross section is compared to the Fontannaz-Guillet-Heinrich (continuous red) and Zotov-Lipatov (dashed blue) calculations.

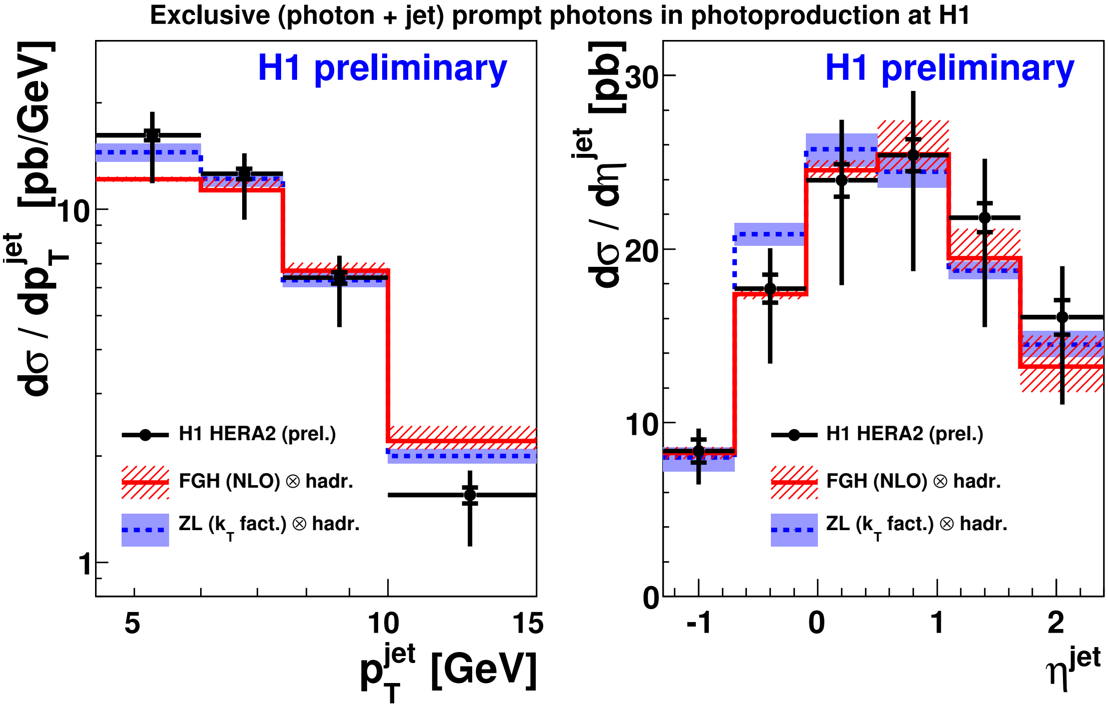

Figure 5: Exclusive prompt photon single differential cross sections as function of p_T^{jet} (left) and η^{jet} (right). The cross sections are measured in range defined in caption of figure 4. The inner errors in the figures represent the statistical errors, while the outer are the statistical and the systematical errors added in quadrature. The measured cross section is compared to the Fontannaz-Guillet-Heinrich (continuous red) and Zotov-Lipatov (dashed blue) calculations.

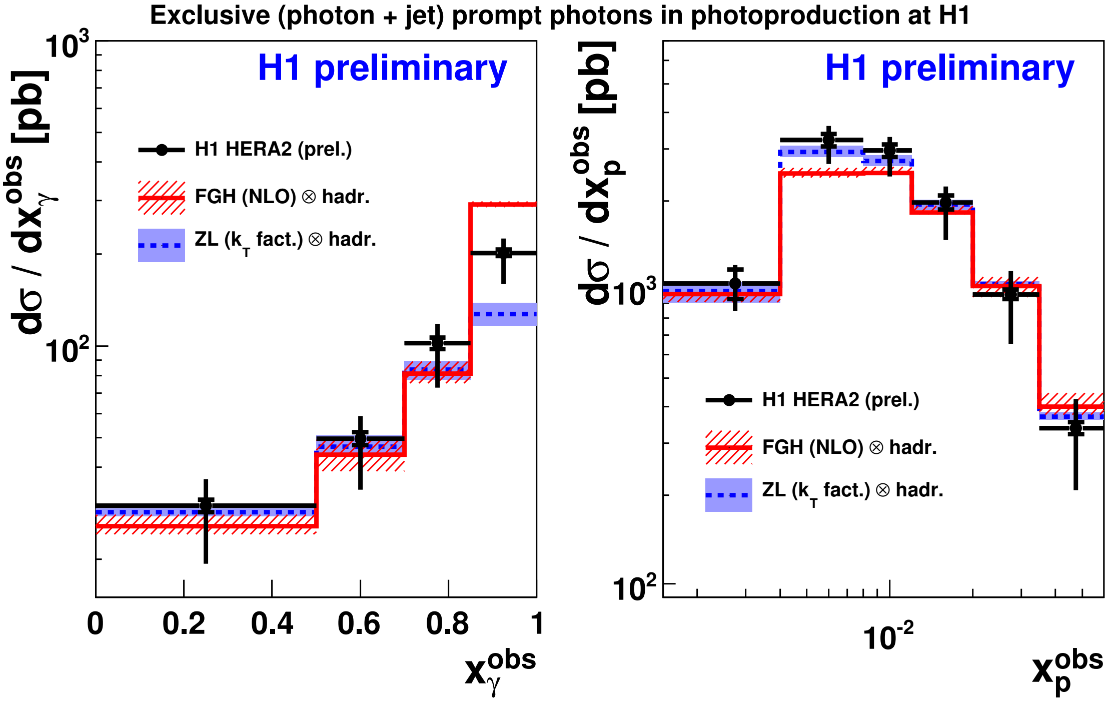

Figure 6: Exclusive prompt photon single differential cross sections as function of x_γ^{obs} (left) and x_p^{obs} (right). The cross sections are measured in range defined in caption of figure 4. The inner errors in the figures represent the statistical errors, while the outer are the statistical and the systematical errors added in quadrature. The measured cross section is compared to the Fontannaz-Guillet-Heinrich (continuous red) and Zotov-Lipatov (dashed blue) calculations.